Discreteness effects on the formation and propagation of breathers in nonlinear Klein-Gordon equations

Thierry Dauxois and Michel Peyrard
Laboratoire de Physique, Ecole Normale Supérieure de Lyon, 46 allée d'Italie, 69007 Lyon, France

C. R. Willis
Department of Physics, Boston University, 590 Commonwealth Avenue, Boston, Massachusetts 02215
(Received 26 May 1993)

Oscillating localized solutions are studied in the case of a nonlinear Klein-Gordon equation, extending previous results. The discreteness effects are studied on the propagation of the breathers and we show that the Peierls-Nabarro potential is an increasing function of the amplitude of a breather. Showing the possible role of impurities to trap the modes in a finite region and results for the collision phenomenon between such excitations, we exhibit a mechanism to localize energy as large-amplitude breathers in the lattices. Their creation is thus explained by a physically relevant mechanism.

PACS number(s): 03.40.Kf, 63.20.Pw, 46.10.+z

I. INTRODUCTION

Solitons, or more generally localized nonlinear excitations, have been used to model many physical phenomena in solids or macromolecules [1], such as dislocations, magnetic-domain walls, collective electronic [2] or ionic [3] charge transport in solids or macromolecules, energy transport in proteins [4], or the local opening of DNA [5,6]. In most of these applications, the atoms or spins can be considered as harmonically coupled and subjected to a nonlinear external potential which can be due to the rest of the crystal or macromolecule (such as in dislocations, ferroelectric domain walls, DNA dynamics) or an external field (such as in magnetic chains). This results in a nonlinear Klein-Gordon equation for the on-site degree of freedom u_n of the form

$$\ddot{u}_n - (u_{n+1} + u_{n-1} - 2u_n) + \frac{\partial V}{\partial u}(u_n) = 0,$$

where V is an external (substrate) potential.

Although in the mentioned cases [1], the physical system of interest is a discrete lattice, the theoretical modeling generally uses a continuum limit approximation to allow for analytical treatment. The role of discreteness to modify the conclusions derived in the continuum limit has been investigated in detail in the case of topological excitations (kinks) that interpolate between two different ground states of the system [7–9].

There is, however, another class of excitations that is important for physical applications: the large-amplitude localized excitations or breathing modes. Contrary to the kinks, which have a finite minimum energy, the breathers, which can be created without an energy threshold, often play the role of precursors in the formation of nonlinear excitations. Although some studies of the role of discreteness on breather dynamics have been performed [6,10–13], the role of the lattice is much less understood for breathers than for kinks. One reason is that breathers are two-parameter solutions that are not only defined by their position but also by their internal dynamics.

Breathers in Klein-Gordon equations are particular cases of intrinsic localized states in anharmonic lattices which have been extensively studied in the last few years [14–17]. However, the models that have been considered in this context involve anharmonic *interactions* between particles, while in the Klein-Gordon models the nonlinearity comes from an *on-site potential*. For the study of discreteness effects on permanent-profile kink solutions, this distinction has been found to be crucial. While narrow kinks in a Klein-Gordon model radiate phonons and therefore lose energy [18], nontopological kinks in monoatomic lattices can propagate without any energy loss [19]. This fundamental difference can be attributed to different linear dispersion relations in the two cases. In other approaches [11–13], the study of the breathers is performed on a discrete nonlinear Schrödinger (NLS) equation. This introduces some constraints related to the properties of the NLS equation; for instance, the conservation of the norm, which imposes a strong restriction on the dynamics of the breathers (for instance, the trapping of the soliton on the *maximum* of a perturbative potential [11]). Although the discrete NLS can be derived with some approximations from the Klein-Gordon equation, this conservation relation does not apply to the original equation. Therefore it is important to study the effects of discreteness on the breather *directly on the Klein-Gordon equation* rather than on the discrete NLS. This is the aim of this paper.

In a previous paper [6], we considered the role of discreteness in the ϕ^3 model. By first studying the equations of motion of the system in the continuum limit, we obtained approximate expressions for the breather solutions. Owing to the importance of breathing motions in many physical applications, and particularly in DNA, we developed a Green's-function method to take account of

the discreteness effects in detail. Searching long-lived oscillatory solutions, we found an accurate expression, and the agreement with the simulation, both qualitative and quantitative, was a strong demonstration of the reliability of the formalism when the extent of the breather was of the order of the substrate lattice spacing. The main conclusion that emerged from our results was that the discreteness of the chain could be of great importance for a model, particularly when breather modes are involved. But this work was confined to the time evolution of harmonic lattices, with nonlinear on-site potential, associated with *static* localized modes. We consider here the propagation of breather modes. We also investigate the *creation* of large-amplitude breathers and show how it can be related to the ability of the breathers to propagate in the lattice and to their properties when they interact. Moreover we study the effect of impurities. The behavior of the breathers in the presence of impurities is interesting in two respects. First it shows the stability of the breathers and second the impurities can trap breathers in some region of the space where their interaction can result in the formation of large-amplitude excitations.

The remainder of the paper is organized as follows. In Sec. II, we present briefly the model and the small-amplitude breathers. Then, in Sec. III, in order to complete the first work [6], we explain the role of discreteness on the propagation. We present a simple formalism to obtain analytical expressions of the solution. We can then obtain the Peierls-Nabarro barrier for a breather. In Sec. IV, we present the interaction of breathers with one or two impurities of the lattice. In Sec. V, we exhibit the combined role of the impurities and the collisions on the discrete breathers to localize energy in the chain.

II. MODEL AND SMALL-AMPLITUDE BREATHERLIKE EXCITATIONS

The discrete ϕ^3 model that we consider is a chain of particles of mass $m = 1$ equally spaced and submitted to the substrate potential

$$V(u) = \begin{cases} \omega_d^2 \left(\frac{u^2}{2} - \frac{u^3}{3} \right) , & \text{if } u \leq 1 \quad (1a) \\ \frac{\omega_d^2}{6} , & \text{if } u \geq 1, \quad (1b) \end{cases}$$

where ω_d^2 is a constant and u the displacement of the particle from its equilibrium position. The potential is then qualitatively analogous to the Morse potential, i.e., a potential with a plateau at large positive displacement, a strong repulsion for the negative ones, and finally a well around the equilibrium position. All the analytical results will be obtained in the region of the well, below the critical value $u = 1$, but it is necessary to modify the ϕ^3 potential for displacements greater than 1, to prevent a possible divergence of the displacements in numerical simulations. Nearest-neighboring particles are harmonically coupled with elastic coefficient unity so that the Hamiltonian of the system is

$$H = \sum_n [\tfrac{1}{2}\dot{u}_n^2 + \tfrac{1}{2}(u_n - u_{n-1})^2 + V(u)]. \quad (2)$$

Therefore, the equations of motion are given by

$$\ddot{u}_n - (u_{n+1} + u_{n-1} - 2u_n) + \omega_d^2 \, (\, u_n - u_n^2) = 0 \, . \quad (3)$$

We are interested in cases where ω_d^2 can be as large as $\omega_d^2 = 10$, so that the continuum limit approximation is not valid and we have to take into account the complete discreteness of the system. Linear oscillations of the chain of frequency ω and wave vector q are described by the dispersion relation

$$\omega^2(q) = \omega_d^2 + 4\sin^2(q/2) \, . \quad (4)$$

The localized modes that we want to investigate are lying below the bottom of the harmonic band ω_d.

As a first step, considering only a weakly nonlinear solution, we can apply the usual multiple scale expansion [20] to provide an asymptotic perturbation expansion in the amplitude of the breather. Following the standard method, we obtain [6] the well-known nonlinear Schrödinger equation for the amplitude:

$$i\frac{\partial F_1}{\partial T} + P\frac{\partial^2 F_1}{\partial S^2} + Q|F_1|^2 F_1 = 0, \quad (5)$$

where the nonlinearity and the dispersion parameter are given by

$$Q = \frac{\omega_d^2}{\omega} \, \frac{5\omega_d^2 + 32\sin^4\left(\frac{q}{2}\right)}{3\omega_d^2 + 16\sin^4\left(\frac{q}{2}\right)}, \quad (6)$$

and

$$P = \frac{\omega_d^2\cos(q) - 4\sin^4\left(\frac{q}{2}\right)}{2\omega^3}. \quad (7)$$

In the large-wave-vector limit, we can then find an approximate solution localized and oscillating in time, which behaves like a breather mode. At first order in a small parameter ϵ, its expression is

$$u_n(t) = 2\epsilon A \operatorname{sech}\left(\frac{n - V_e t}{L_e}\right)\cos(\Theta n - \omega_b t) + O(\epsilon^2), \quad (8)$$

where A, V_e, and L_e are the amplitude, the velocity, and the width of the wave, whereas Θ and ω_b are the renormalized wave vector and frequency of the breather (see the complete expression in the previous paper [6]). This NLS breather gives us an accurate expression for the breathers in the small-amplitude limit.

In the earlier study, we restricted ourselves to static breather modes; here we will focus on the time evolution of propagative ones. The propagation of breather modes involves three time scales, defined by the three following frequencies: the frequency of the breather's oscillation ω_b, the frequency of the phonon's modes ω_d, and the last one, which corresponds to the meeting of the breather with the lattice during the propagation (the last one corresponds to the so-called Peierls Nabarro frequency). Nontrivial combination effects of these three frequencies will be studied in the next section.

III. PEIERLS-NABARRO BARRIER FOR A BREATHER

A. Propagation of small-amplitude breathers

The breathers obtained with the method discussed above are sufficiently stable to have a long lifetime that

gives them sufficient time to interact, provided that they can move in the lattice. This point is not as trivial as it might seem if one has in mind the picture of solitonlike excitations in a continuum medium because discreteness breaks the translational invariance. The evolution of the position of the breathers is shown in the small-amplitude case in Fig. 1(a) and in the medium case in Fig. 1(b). It is not easy to determine precisely the center of the pulse; however, if we use a parabolic approximation for the pulse, we obtain a good approximation. If n is the index of the maximum of the pulse, and $(n+1)$ and $(n-1)$ the index of its two neighbors, the position of the center of the excitation is

$$X_M = n + \frac{u_{n-1} - u_{n+1}}{2(u_{n+1} + u_{n-1} - 2u_n)} . \tag{9}$$

This expression allows us to follow the position of the breather and to distinguish here two strongly different behaviors. When the amplitude is very small, the excitation can move without difficulties. A precise analysis of the shape of the excitation shows that, during its propagation, the solution adapts itself to the real potential, since the initial condition obtained with the semidiscrete approximation is not exact. But, when the breather has a medium amplitude, we note that the excitations are trapped on one site, more or less quickly, according to the initial speed. The comparison of the two figures shows that the propagation of the modes is more difficult when their amplitude is bigger.

The trapping effect of the discreteness is well known for topological solitonlike excitations and has been extensively investigated in the context of dislocation theory [21]. In a lattice, a kink cannot move freely. The minimum energy barrier that must be overcome to translate the kink by one lattice period is known as the Peierls-Nabarro (PN) barrier, E_{PN}. It can be calculated by evaluating the energy of a static kink as a function of its position in the lattice. For the various models that have been investigated, two extremal values are generally obtained when the kink is exactly situated on a lattice site (centered solution) or when it is in the middle between two sites (noncentered solution).

For a discrete breather very little is known, although the PN barrier has been shown to exist [22]. One of the difficulties is that the breather is a two-parameter solution. While, for a kink, the PN barrier depends only on discreteness, i.e., on the model parameters, for a breather it depends also upon its amplitude (or frequency). This amplitude dependence is crucial for our analysis because we are interested in the growth of breathers. As they increase in amplitude, the PN barrier that they feel changes. The definition of the Peierls barrier itself is not as simple for a breather as for a kink. In principle, its value can be obtained by monitoring the breather as it is translated along one lattice constant. While for a kink the path followed by the particles in the multidimensional phase space of the system can be obtained by minimizing the energy while the position of the central particle is constrained in all intermediate states, in the case of the breather, the path in the phase space is not a minimum energy path but a succession of saddle points. The energy of a kink which is exactly centered on a site or in the middle between two sites is defined without ambiguity. For a breather with a given frequency, when it is centered on a site, there is no obvious constraint that imposes that it should have the same frequency when it is situated in the middle between two sites. We have used, as a working definition of the PN barrier for a breather, the difference between the energies of a centered and a noncentered breather *with the same frequency*. This definition gives results that agree with the observations of

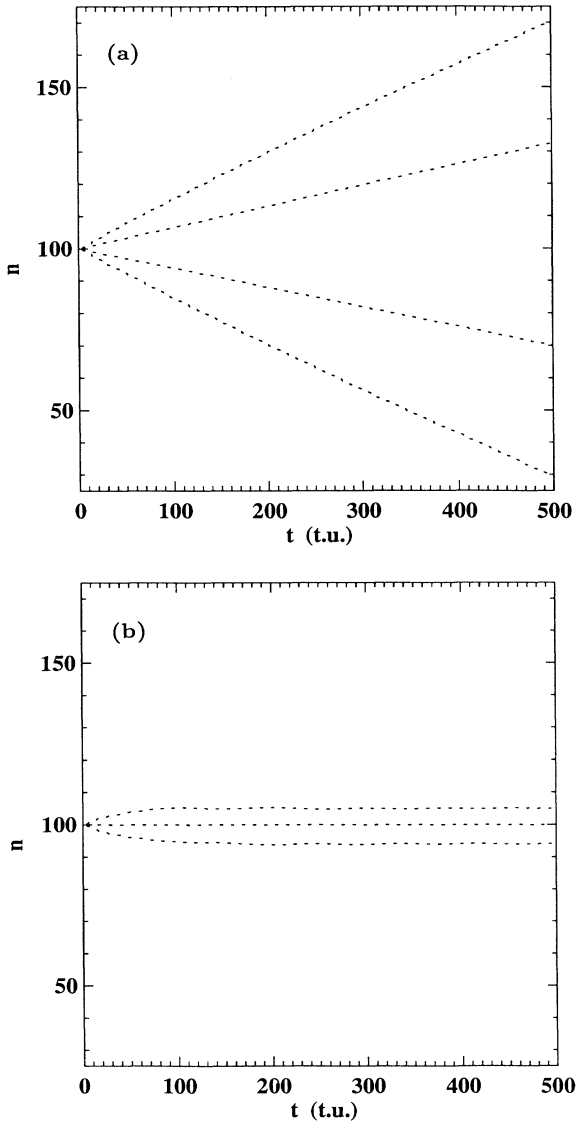

FIG. 1. Position of the center of the breather for different initial speeds. Time units are denoted (t.u.). We present the evolution of the NLS breather with an amplitude of 0.33 in (a) and 0.58 in (b), for the four following initial speeds: $V_e = -1.8\ 10^{-2}$, $V_e = 8.2\ 10^{-2}$, $V_e = 0.182$, and $V_e = 0.282$. Note that in (b), in the second and third cases, the breather is trapped on site 100, which results in the same line in the figure.

the breather motion made by molecular dynamics simulations, but the notion of the PN barrier for a breather will require further analysis.

B. Large-amplitude breathers

To calculate the PN barrier, we have to compare the energy between two cases: the breather is centered on a particle or between particles. In the previous paper [6], we focused our study on the first case, but we can easily extend the method to the second one. The procedure is the following: we look for stationary-mode solutions by putting

$$u_n = \sum_{i=0}^{\infty} \phi_n^i \cos(i\omega_b t) , \tag{10}$$

where ω_b is the eigenfrequency of the breather and ϕ_n^i are the time-independent amplitude of the ith mode. Inserting the *Ansatz* (10) in Eq. (3), we set the coefficients of $\cos(i\omega_b t)$ equal to each other, retaining only the first three terms. We obtain

$$\omega_d^2\, \phi_n^0 - \left[\phi_{n+1}^0 + \phi_{n-1}^0 - 2\phi_n^0\right] = \omega_d^2 \left[{\phi_n^0}^2 + \frac{{\phi_n^1}^2 + {\phi_n^2}^2}{2}\right], \tag{11a}$$

$$(\omega_d^2 - \omega_b^2)\, \phi_n^1 - \left[\phi_{n+1}^1 + \phi_{n-1}^1 - 2\phi_n^1\right] = \omega_d^2 \left[2\phi_n^0 + \phi_n^2\right] \phi_n^1, \tag{11b}$$

$$(\omega_d^2 - 4\omega_b^2)\, \phi_n^2 - \left[\phi_{n+1}^2 + \phi_{n-1}^2 - 2\phi_n^2\right] = \omega_d^2 \left[2\phi_n^0\phi_n^2 + \frac{{\phi_n^1}^2}{2}\right]. \tag{11c}$$

Then, invoking the Green's functions for the linear left-hand sides, we get a set of simultaneous nonlinear eigenvalue equations determining the eigenfrequency ω_b and the eigenfunctions ϕ_n^i:

$$\phi_n^0 = \sum_m G(n-m,0) \left[{\phi_m^0}^2 + \frac{{\phi_m^1}^2 + {\phi_m^2}^2}{2}\right], \tag{12a}$$

$$\phi_n^1 = \sum_m G(n-m,\omega_b) \left[2\phi_m^0 + \phi_m^2\right] \phi_m^1, \tag{12b}$$

$$\phi_n^2 = \sum_m G(n-m,2\omega_b) \left[2\phi_m^0\phi_m^2 + \frac{{\phi_m^1}^2}{2}\right], \tag{12c}$$

where the Lattice Green's functions have the following expression:

$$G(n,\omega_b) = \frac{\omega_d^2}{N} \sum_q \frac{e^{iqn}}{\omega_d^2 - \omega_b^2 + 2[1-\cos(q)]} . \tag{13}$$

For solving this system, the procedure requires more care than in the centered case [6], to avoid the problem of instability of this mode. Indeed, since the position at the top of the PN barrier is intrinsically unstable, regardless of other possible causes of instability, even starting with a symmetrical initial condition, the results show that in all cases the breather moves so that the center reaches the bottom of the well; i.e., the solution converges toward the more stable breather. To prevent this tendency we chose to impose the symmetry and calculate the solution for only a half of the chain, the second half being known by symmetry: thus the position of the breather is fixed. Self-consistently solved, the system (12) give us the values of the breather's frequency and of the amplitude of the different sites.

In Fig. 2(a), we plot the frequency versus the ampli-

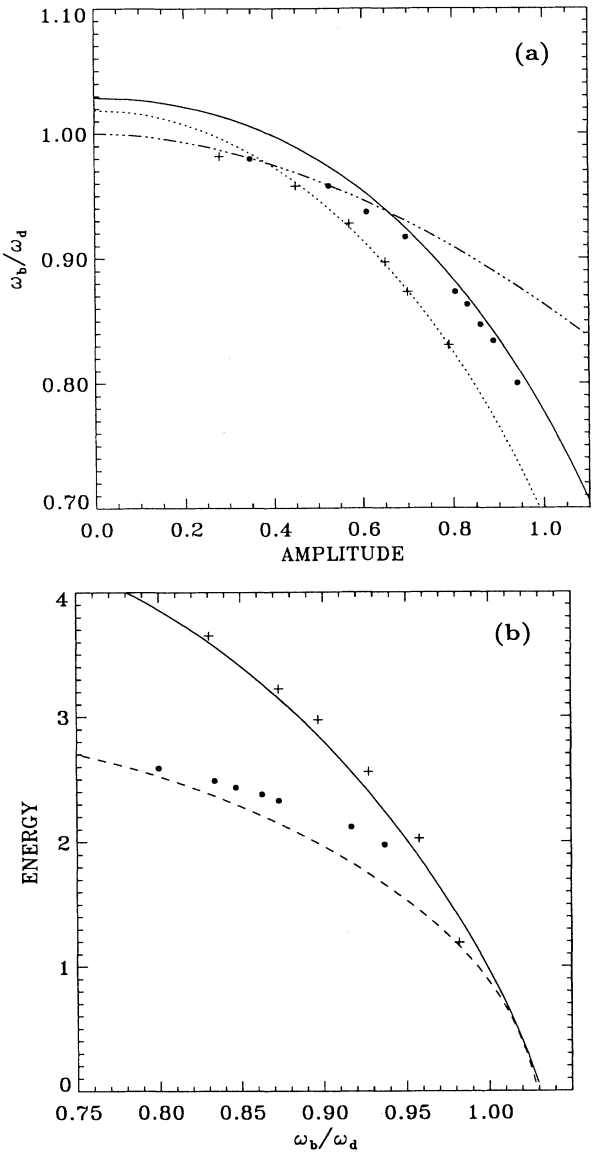

FIG. 2. Comparison of the centered and decentered breathers. (a) Frequency of the breather modes vs amplitude. The solid line refers to Eq. (26), the dotted line to Eq. (30), and the dash-dot-dot-dotted line to the NLS approximation. (b) Total energy as a function of the frequency. The circles (the plus signs) correspond to the solution obtained with the Green's function technique when the breather is centered on a particle (between two particles).

tude for the two modes. At high frequency (i.e., low amplitude), the two curves are very close to each other. As one might expect (see Fig. 3), the amplitude of the mode centered on a particle is larger than when the mode is centered between particles. A comparison of the energies in the two cases reveals a great difference, as shown in Fig. 2(b). The solution centered on a particle has a much lower energy. Indeed, as the discreteness effects are important, the substrate energy is the dominant contribution to the total energy. When the breather is centered between particles, two of them participate mainly in the excitation, giving rise to a substantial increase of the energy, in comparison with the previous case, where only one particle has a large amplitude.

Figure 4 illustrates the simulation of the dynamics of the breather with a decentered solution as an initial condition. The numerical scheme for solving the nonlinear equations of motion (3) is a fourth-order Runge-Kutta method of a lattice with typically 256 atoms and periodic boundary conditions. Starting with a breather centered between sites 24 and 25, and with a frequency $\omega_b = 0.93\ \omega_d$, Figs. 4(a), 4(b), and 4(c) show the envelope of the oscillations of the particles 24, 26, and 25. It is clear that after about 70 breather oscillations, the excitation moves to be centered on particle 25. Although we start with a perfect symmetrical initial condition centered between particles, because of its intrinsic instability, some unavoidable numerical errors have moved the breather down the PN barrier. As the initial condition is clearly not the exact solution at the bottom of the well, a phenomenon of modulation appears: it is a consequence [6] of the combination of the breather's frequency ($0.88\ \omega_d$ after the displacement of the breather) with the

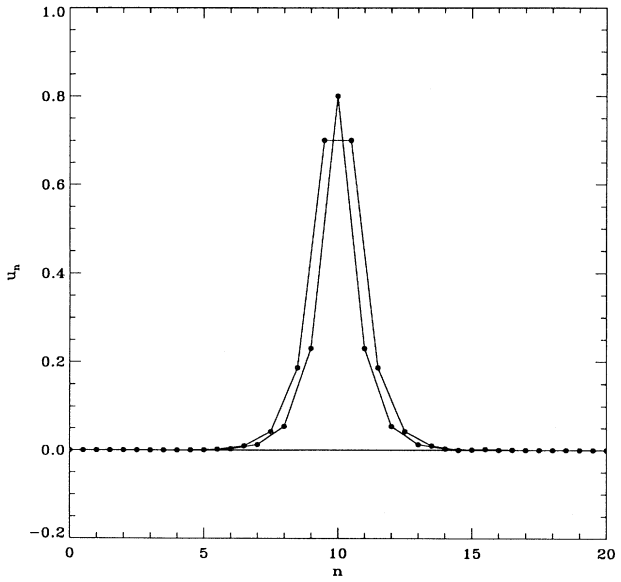

FIG. 3. Profiles of the solutions calculated with the Green's-functions method when the frequency of the oscillations is $\omega_b = 0.873\ \omega_d$. Two cases are shown: the breather centered on a particle or between two particles.

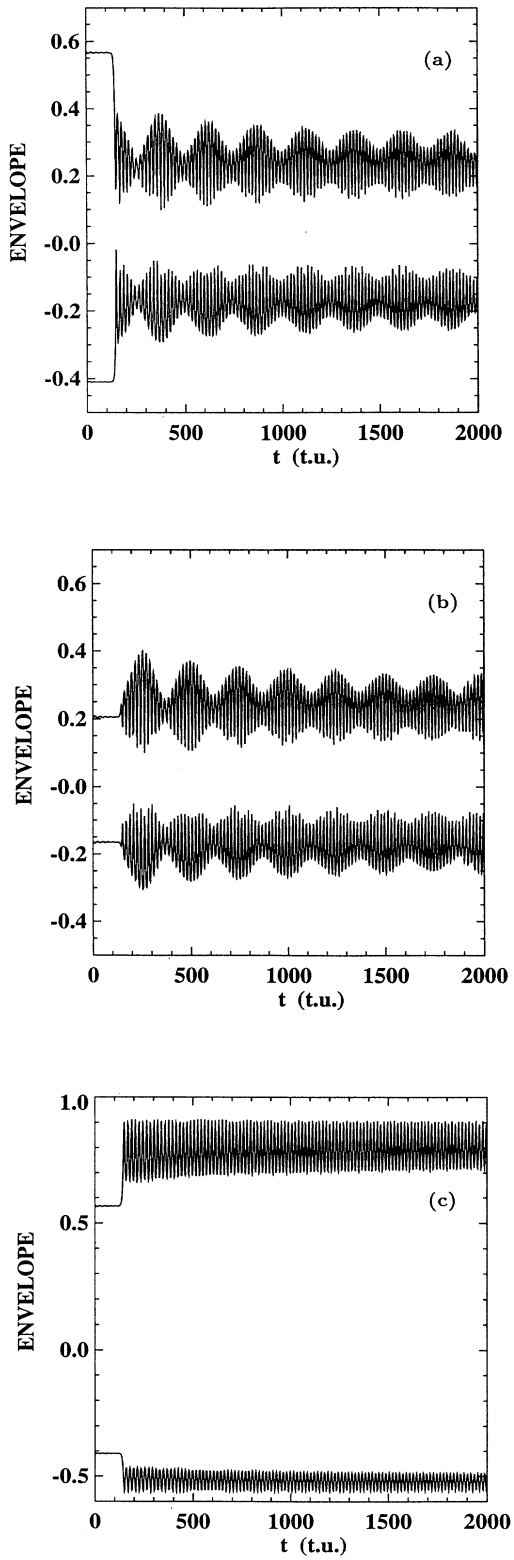

FIG. 4. Envelope of the oscillations of particles 24 (a), 25 (c), and 26 (b), when the breather is centered between particles 24 and 25, at the beginning of the simulations. After about 300 breather oscillations, the excitation moves down to the Peierls-Nabarro well.

mode situated exactly at the bottom of the phonon band, which cannot be radiated away because of its zero group velocity.

Figures 4(a) and 4(b) show the oscillations of the two nearest neighbors of the center. It is clear that, after the translation of the center, they have a similar evolution, except that a new modulation effect is present: it is due to the combination of the former frequency with the frequency of the oscillation in the well of the PN barrier. Furthermore, the two particles are not in phase, because when one starts with a breather, the shape mode (the derivative with respect to the position of the breather's center) is odd; so, with the center on a particle, the shape mode is such that the central site does not move, but the two neighboring sites are 90° out of phase.

As the spontaneous evolution of a decentered breather with a frequency ω gives a centered breather with a lower frequency, we cannot calculate the PN barrier from such a simulation. Although the energy of the system is conserved during the integration of the equations, it does not stay localized in the excitation, since the movement of the breather generates a strong radiation of phonons. The Peierls barrier can be obtained from a calculation of the energy of the solutions given by the Green's-function method, independently in the two cases. Figure 2(b) shows that the PN barrier is very high; as it is an increasing function of the amplitude of the breather [see Fig. 2(a)], the barrier is an increasing function of the amplitude. A small-amplitude breather will propagate easily along the chain, whereas the large-amplitude ones will be trapped on a site because of the additional potential due to the discreteness.

C. Approximate analytical expression and the PN barrier

The Green's-function method provides a very accurate expression for the discrete breather modes, but the solution is known only numerically. When the breathers are highly localized, it is possible to derive an approximate analytical solution for the frequency of the mode versus their amplitude in the two cases. First, we consider the centered case where the mode is on a particle that we call $n = 0$. As the mode is highly localized, we assume $|u_n| \ll |u_1|$ for $|n| > 1$. We seek an approximate solution of Eq. (3), by looking for a solution that is localized over only three sites, putting [17]

$$u_0 = A + B\cos(\omega_b t), \tag{14}$$

$$u_1 = u_{-1} = C + D\cos(\omega_b t)\ , \tag{15}$$

$$u_l = 0 \ for\ |l| \geq 1\ . \tag{16}$$

The dc parts of the ansatz are positive because of the asymmetry of the potential. We insert this ansatz into Eq. (3), and set the coefficients of $\cos(\omega_b t)$ and the constant term equal to each other. We obtain for $n = 0$,

$$0 = 2(C - A) - \omega_d^2\left(A - \frac{B^2}{2} - A^2\right), \tag{17}$$

$$-\omega_b^2 B = 2(D - B) - \omega_d^2(B - 2AB). \tag{18}$$

For $n = 1$, it yields

$$0 = A - 2C - \omega_d^2\left(C - \frac{D^2}{2} - C^2\right), \tag{19}$$

$$-\omega_b^2 D = B - 2D - \omega_d^2(D - 2CD). \tag{20}$$

As the excitation is rapidly decreasing, we can estimate that $A \gg C$; Eq. (17) gives then

$$B = \sqrt{2A\left(\frac{2}{\omega_d^2} + 1 - A\right)}\ , \tag{21}$$

whereas (18) and (20) give

$$\omega_b^2 = 2\left(1 - \frac{D}{B}\right) + \omega_d^2(1 - 2A) \tag{22}$$

$$= 2 - \frac{B}{D} + \omega_d^2(1 - 2C). \tag{23}$$

Neglecting C in (23), we obtain from these two equations,

$$\left(\frac{D}{B}\right)^2 + \omega_d^2 A\ \left(\frac{D}{B}\right) - \frac{1}{2} = 0\ . \tag{24}$$

Then, we get

$$\frac{D}{B} = \frac{-A\omega_d^2 \pm \sqrt{(A\omega_d^2)^2 + 2}}{2}\ . \tag{25}$$

As we are interested in breather modes, the particles should oscillate in phase: the ratio D/B must be positive and that is why we keep only the plus sign. Equation (23) gives then

$$\frac{\omega_b^2}{\omega_d^2} = \frac{2}{\omega_d^2} + 1 - A - \sqrt{\frac{2}{\omega_d^4} + A^2}. \tag{26}$$

Consider now the case where the center of the excitation is between two particules [in our notation, between the site (-1) and (0)]. We take the similar ansatz with two unknown functions $u_0 = u_{-1}$ and $u_1 = u_{-2}$. Now we obtain the two following equations for the case $n = 0$:

$$0 = (C + A - 2A) - \omega_d^2\left(A - \frac{B^2}{2} - A^2\right), \tag{27}$$

$$-\omega_b^2 B = (B + D - 2B) - \omega_d^2(B - 2AB). \tag{28}$$

An analysis similar to that given above can be carried out, and we obtain

$$\frac{D}{B} = \frac{-(1 + 2A\omega_d^2) + \sqrt{(1 + 2A\omega_d^2)^2 + 4}}{2} \tag{29}$$

and

$$\frac{\omega_b^2}{\omega_d^2} = \frac{3}{2\omega_d^2} + 1 - A - \sqrt{\frac{1}{2\omega_d^4} + \left(\frac{1}{2\omega_d^2} + A\right)^2}. \quad (30)$$

The comparison of the two equations (26) and (30), with the results of the Green's-function method is shown in Fig. 2(a). As might be expected at low amplitude, the results tends to the NLS case, with a good agreement. In this domain, as the excitation concerns more than three or four particles, contrary to the postulate in the *Ansätze* (14) and (15), the present formalism failed and the agreement is poor. But, in the highly localized regime, in which we are essentially interested, the two expressions given by the simple *Ansätze* are valid. Although the method can seem very crude, it provides accurate results in the very discrete cases, because the solutions are naturally well localized, so that the displacements, which are ignored here, are really very small.

Using these results we can obtain the energy of the mode. The expression for the case centered between particles is

$$E_c = \tfrac{1}{2}u_1^2 + (u_1 - u_0)^2 + \omega_d^2\left(\frac{u_0^2}{2} - \frac{u_0^3}{3}\right) + 2\omega_d^2\left(\frac{u_1^2}{2} - \frac{u_1^3}{3}\right) \quad (31)$$

and

$$E_d = E_c + \omega_d^2\left(\frac{u_0^2}{2} - \frac{u_0^3}{3}\right) \quad (32)$$

in the other case, where the expressions of the two displacements u_0 and u_1 are easily determined, using A, B, C, and D. The results shown in Fig. 2(b) attest that, despite its simplicity, the calculation gives accurate results, especially in the second case.

IV. IMPURITIES

We have shown the possible existence, in the lattice, of very narrow breathers with a spatial extent limited to a few lattice spacings. As their spatial extensions are so small, we can expect them to interact strongly with isolated impurities in the lattice. In this section, we study this impurity effect, which has an intrinsic interest because in a physical system impurities are likely to be present, and, as shown in the next section, a possible role in the creation of large-amplitude breathers.

That defect, which we have chosen, is a site without substrate potential. In our DNA model [23], such a site corresponds to a position where the H bonds connecting two bases in a pair are broken. The solvent effects could be at the origin of such a defect: some experiments about hydrogen bonds have shown that, in water, they can be broken easily at temperatures well below the denaturation temperature. This phenomenon is present in the macromolecule because of water molecules around the DNA skeleton; as the substrate potential is a model of these interactions, we will study the propagation of breathers in a chain with such a defect. Our approach is the following: first, we will obtain the expression of the impurity mode in the linear limit. Then we will prove that this limit is relevant for this study and we will be able to deduce the behavior of a breather in the presence of such a defect. Finally, in Sec. V, we use this result in order to propose a mechanism of energy localization.

A. Defect mode

We call the particle with the broken bond the origin $n = 0$. The equations of motion are now

$$\ddot{u}_n - (u_{n+1} + u_{n-1} - 2u_n) + \omega_d^2(1 - \delta_{0,n})(u_n - u_n^2) = 0. \quad (33)$$

In the linear approximation, we consider the Green's function G, which satisfies the matrix equation

$$(\omega^2 - M)\, G = 1 \quad \text{where} \quad M = \left[\frac{\partial^2 H}{\partial u_n \partial u_m}\right]. \quad (34)$$

Denoting with the index 0, the homogeneous case, the matrix equation produces the chain of equations $G_0(i,j) = G_0(|i-j|)$.

We have then

$$(\omega^2 - \omega_d^2 - 2)\, G_0(0) = 1 - 2G_0(1), \quad (35)$$

$$(\omega^2 - \omega_d^2 - 2)\, G_0(1) = -[G_0(0) + G_0(2)], \quad (36)$$

whose solution [24] is $G_0(n) = A\, y^{|n|}$, with

$$y = -x - \sqrt{x^2 - 1},$$

$$A = \frac{-1}{2\sqrt{x^2 - 1}},$$

and

$$x = \frac{\omega^2 - \omega_d^2 - 2}{2}.$$

Now taking into account the impurity at the origin, with $M = M_0 + \delta M$, we obtain $\delta M(0,0) = -\omega_d^2$. Using the Dyson equation [25]

$$G = G_0 + G_0\, \delta M\, G, \quad (37)$$

we can obtain the expression of the Green's function for the imperfect chain:

$$G(0,0) = \frac{G_0(0)}{1 - \delta M(0,0) G_0(0)}. \quad (38)$$

As the zeros of the denominator give the spectrum of the chain with the impurity, we find that the linear impurity mode (TM) will occur with the frequency:

$$\omega_{\mathrm{IM}}^2 = \omega_d^2 + 2 - \sqrt{4 + \omega_d^4}. \quad (39)$$

Therefore the local mode is in the gap, and with our parameter the breather frequency is in the lower half of the frequency gap.

The calculation of the shape and the frequency of the mode was obtained in the linear approximation, but as the Green's function G is a rapidly decreasing function, the pulse is extremely localized around the impurity. If the center of the excitation has an amplitude of 1, the first neighbors will have an amplitude lower than 0.1, where the linear approximation is really valid. Furthermore, as the equation of motion of the center of the mode is linear, since on this site the nonlinear substrate potential is suppressed, no corrections should be done for this particle. Numerical simulations of the dynamics of this mode have confirmed that the solution is indeed extremely accurate.

B. Interaction of breathers with impurities

Having checked numerically the existence of the impurity mode, the question arises as to how it can help us to localize the energy. As the high-amplitude breather modes of Sec. III have a significantly higher frequency, and as the phonons of the chain have a frequency gap ω_d, they will have extreme difficulty in getting by the IM, except due to some very nonlinear phonon process that will end up with the frequency of the IM. This property will be useful in trapping excitations in a region. Indeed, if two impurities of this type are located on the chain, the energy between them will be trapped. Putting an oscillatory solution of the phonon type between two sites, the excitation stays located in that region, and is not radiated away as it does without impurities: the energy is clearly trapped. Now suppose that one puts a moving breather in that region whereas it should propagate along the chain as in Sec. II, the excitation is now trapped, because of successive reflections on the impurities, as shown by Fig. 5(a). We clearly see the oscillatory motion of the excitation between the two impurities, located on sites 30 and 70.

But this result was obtained at zero temperature, and the propagation of breathers has to be checked in the presence of small perturbations. In order to study this aspect, we have investigated the dynamics of the model in contact with a thermal bath by molecular dynamics simulations with the Nosé scheme [23,26]. The system is aged for 150 000 time steps ($\simeq$ 300 oscillations of the breather) to reach thermal equilibrium at 100 K. Then the breather solution is added to the system and the simulation is then performed without a thermal bath at constrained energy.

Figure 5(b) shows the evolution of the energy of the system by a contour plot versus the unit cells and time. As there are two impurities in sites 30 and 70, the localized structure has an oscillatory motion between these two "walls." We can also check that the density of small fluctuations is bigger in the trapped region, because the linear waves could not escape from this region. If we can notice that the propagation of the breathers is modified because of fluctuations, we note that they stay localized in spite of the many collisions with the impurities and with the fluctuations. The breather is therefore stable enough to be an important excitation in the physics of the system.

But now arises the main question: How is it possible to create such an oscillation requiring an important localization of energy? The small-amplitude breathers can easily be created by thermal fluctuations, as we noticed in a very similar model [6]. But the energy of large-amplitude breathers is very large, and it is necessary to find how their creation is possible to justify their existence and then their importance. In the next section,

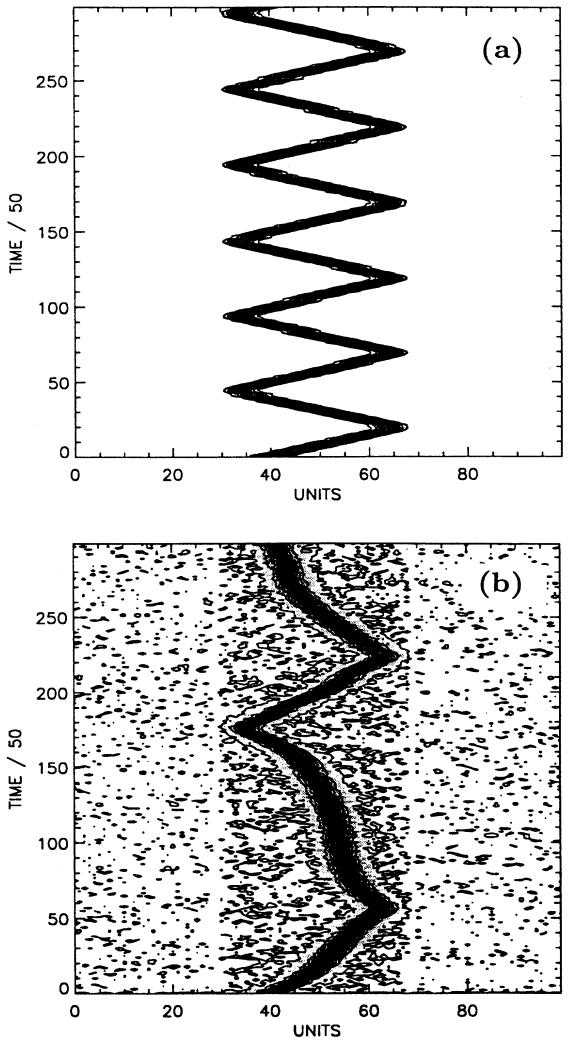

FIG. 5. Propagation of a NLS breather in the chain with two impurities, illustrated by the contour plot of the energy per site vs the maximum of the breather's oscillation. The two figures correspond to the evolution during 15 000 time units and we plot only a part of the whole chain. The two impurities (broken bond) are located on sites 30 and 70. The breathers correspond to Eq. (2.7) of Ref. [6] with the parameters $u_e = -0.13$, $q = 0.2$, and $A = 0.15$. (a) Propagation at zero temperature. (b) Propagation of the breather in a chain thermalized at $T = 100$ K.

we will present a possible mechanism which gives rise to large oscillating excitations.

V. LOCALIZATION BY COLLISIONS

The existence of localized solutions of the equations of motion is not sufficient for their physical relevance. They must be *created* by some mechanism in the system of interest. In this section, we focus our attention on the *formation* of large-amplitude breathing modes, and we show that discreteness is not only essential for their stability, it provides a mechanism, alternative to modulational instability, for their formation. This channel for energy concentration, which is specific to lattices, is not sensitive to the details of the nonlinear lattice model which is considered. Therefore it appears as a very general process leading to localization of energy in a lattice.

The first step toward the creation of localized excitations can be achieved through modulational instability, which exists in a lattice as well as in a continuum medium, although discreteness can drastically change the conditions for instability [27] (e.g., at small wave numbers a nonlinear carrier wave is unstable to *all* possible modulations of its amplitude as soon as the wave amplitude exceeds a certain threshold). However, the maximum energy of the breathers created by modulational instability is bounded because each breather collects the energy of the initial wave over the modulation length λ, so that its energy cannot exceed $E_{\max} = \lambda e$, where e is the energy density of the plane wave. Consequently, although modulational instability can lead to a strong increase in energy *density* in some parts of the system, it cannot create breathers with a *total* energy exceeding $E_{\max}$. For a given initial energy density, one can however go beyond this limit if one excitation can collect the energy of several breathers created by modulational instability. Such a mechanism is not observed in a continuum medium because there the breathers generated by modulational instability are well approximated by solitons of the nonlinear Schrödinger equation, which can pass through each other without exchanging energy.

It is easy to check that two small-amplitude breathers could go through each other, keeping their shape. The ability of solitons to survive collision completely unscathed is frequently used as an identifying characteristic in experimental and numerical investigations to separate solitons from a large panorama of signals. When the approximations used to obtain this equation are valid, the envelope solitons collide without interference. In contradiction, when the amplitude increases, the limit is less valid and the excitations collide inelastically. In our case, the large-amplitude breather modes do not go through each other without interactions because of discreteness effects. Qualitatively, the collision of two breathers with different amplitudes increases the difference. This process could be a realistic mechanism of the large-amplitude breathers' creation, since *the exchange tends to favor the growth of the larger excitation.*

Indeed, as a breather with a medium amplitude grows at each collision with a smaller one, it needs to collide with a few of them to have a bigger amplitude. The process is faster when the excitation is trapped between two impurities, because of the different reflections, if there are many excitations in the trapping region, the collisions take place until the main excitation has absorbed the energy of the others. Figure 6(a) shows this mechanism. We start the simulation with two different breathers located between two impurities. At the beginning, the bigger one is on site 40; it collides many times with the smaller one, which started from site 60. We note that the amplitude of the first one increases, whereas the other one decreases. Finally, the process gives rise to only one excitation, with a large amplitude and a frequency in

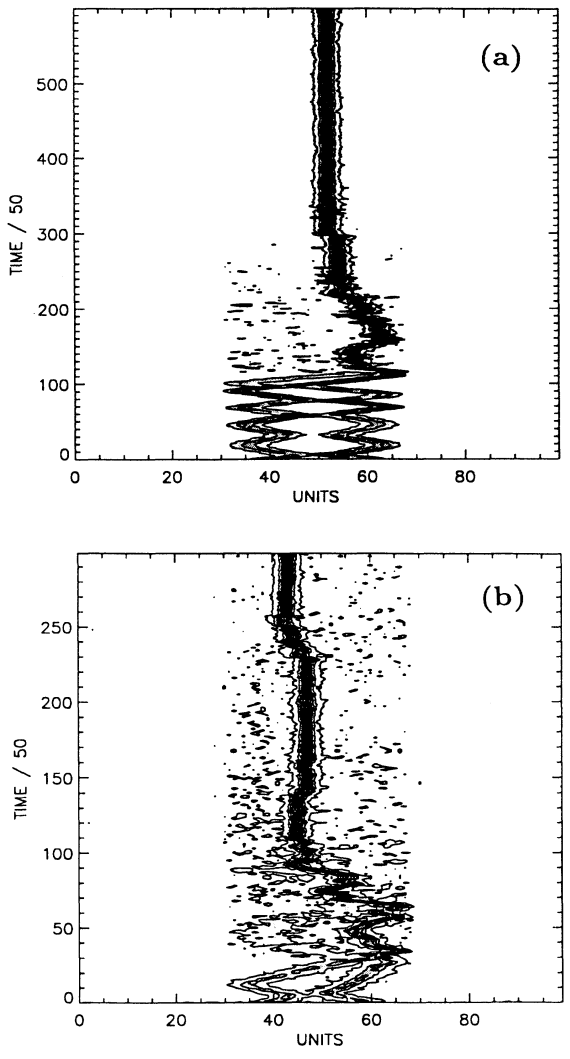

FIG. 6. Propagation of two NLS breathers in the chain with two impurities: the same as in Fig. 5, centered on site 40 at the beginning of the simulation, and a smaller one ($A = 0.11$) on site 60. The picture illustrates the contour plot of the energy per site vs the maximum of the breather's oscillation. Two impurities (broken bond) are located on sites 30 and 70. (a) Propagation at zero temperature. (b) Propagation of the breather in a chain thermalized at $T = 100$ K.

the phonons' gap. We note also that the final excitation does not propagate along the chain, since the PN barrier is too large, and that some small excitations are radiated away during the few collisions and cannot escape from the trapping region. They disappear because they are absorbed by the main excitation.

Figure 7 presents the evolution of the energy of the main breather versus time. Because of the difficulty in defining the limits of the breather, we decided to consider the energy of three sites: the center of the breather and its two neighbors. After smoothing the data in order to reduce the fluctuations due to the definition of the energy, we see clearly that the energy increases as a function of time. A careful analysis shows that the energy increases by step at each collision. It is clear, according to the picture, that the bigger the difference between the two breathers, the stronger the transfer in energy. We have checked that the difference in the phases of the two excitations changes the energy transfer; but qualitatively, once more, the system gives rise to only one excitation, more or less rapidly: it is one of the large-amplitude breathers, which expression was given in Sec. III. As the Fourier transform of the breather oscillations give a frequency in the phonons' gap ($\omega_b = 0.96\ \omega_d$), the excitation does *not* emit radiations that could give rise to a small damping of the breather (this is correct to lowest order since the harmonics generated by the nonlinearity could be in the phonons' band and radiations could be emitted).

For applications to a real system, it is important to check that the result subsists in the presence of thermal fluctuations. Figure 6(b) confirms this result in a thermalized chain. As for Fig. 5(b), the system was simulated with the Nosé scheme, so that we can consider the system to be in equilibrium, in the sense of the canonical ensemble, at a fixed temperature. Then the two breathers were added, and the figure shows the evolution of the two breathers with fluctuations. If the dynamics is of course modified, we note that, qualitatively, the system evolves in the same way: we obtain only one big breather, which is static because of its big amplitude. Some other simulations with other temperatures have confirmed that this creation process is really relevant in this model, even with fluctuations.

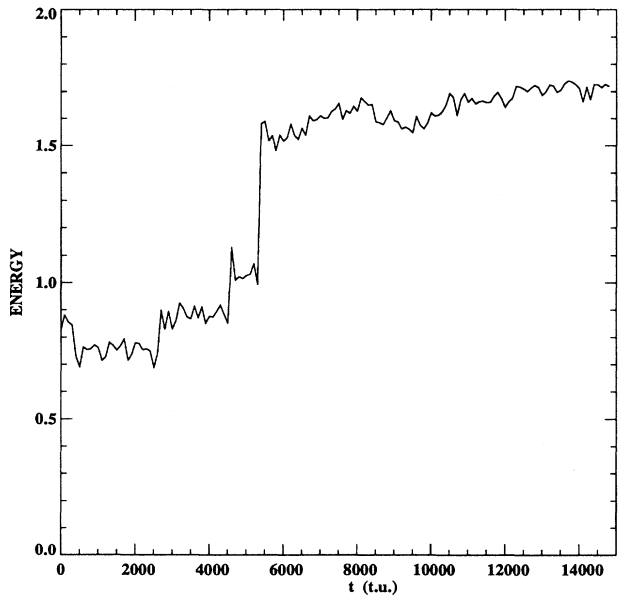

FIG. 7. Evolution of the energy of the three main particles of the bigger breather as a function of time.

In fact, we observe that its growth rate is larger in the presence of thermal fluctuations, because it collects some energy from the fluctuations. The results do not depend on the boundary conditions. Multiple collisions can also be generated by periodic boundary conditions and the same results are found. More importantly, the results do not depend on the particular nonlinear lattice model that is considered. Using the more physical Morse potential instead of $V(u)$ given by Eq. (1) leads to the same general conclusions. However, the process contains also its own regulation mechanism because of the fast increase of the Peierls barrier with the amplitude of the breathers. When they become large enough, the breathers stay trapped by discreteness. As a result, energy initially evenly distributed over the lattice tends to concentrate itself into large-amplitude breathers, but the localization stops before all the energy has collapsed into a single very large excitation.

VI. CONCLUSION

In this paper, we have extended our previous work on static large-amplitude breathers to propagating ones. Since the Peierls-Nabarro barrier is an increasing function of the amplitude of the breather, we showed that these breathers will have difficulties moving. Then we showed that the impurities could trap the excitations in a small region. Finally, we have presented a simple mechanism that could explain the creation of large-amplitude breathers. The energy of the small-amplitude breathers being small, it is reasonable to consider that they are easily created by thermal fluctuations, and numerical simulations at constrained energy have confirmed [23] this picture. Once these excitations are present, since they are not solitons in the strict sense, their collisions give rise to excitations with an increasing amplitude. Although the impurities are not essential, they accelerate the mechanism by multiplying the number of collisions between the excitations. Finally, we therefore obtain localized excitations with a large amplitude, which are extremely stable.

Owing to the importance of breathing motions in many physical applications and particularly in DNA, it was very important to explain the creation process of these excitations. We showed that it is closely related to the discreteness of the lattice. Indeed, first, the breather modes are stable only in the discrete system; second, the collisions of two excitations present an antidemocratic behavior which increases the bigger excitation, contrary to the results found in the continuum limit of nonlinear system. The frequency of the breathers is a decreasing function of the amplitude of the excitation. As their energy

increases because of the collision process, their frequency decreases until it reaches the zero value where the excitations do not breathe anymore, but stay open. This simple mechanism could be of great importance to explain how localized bubbles could be generated in physical systems without external driven force.

It is important to notice that discreteness acts simultaneously to *stabilize* the breathers and to *cause their growth.* Therefore, as the two aspects work in synergy, the existence of large-amplitude excitations in nonlinear *lattices* is likely to occur in many physical systems. Intrinsic localized modes have been found in more than one dimension [28,29]. It would be interesting to study their interaction in the very discrete case to see whether the same mechanism for their growth is possible. Similarly, the case of magnetic systems would be interesting to study in the same spirit.

ACKNOWLEDGMENTS

T.D. and M.P. acknowledge the hospitality of the Center for Nonlinear Studies of the Los Alamos National Laboratory where part of this work has been done. The authors wish to acknowledge the Advanced Computing Laboratory of Los Alamos. This work was performed on computing resources located at this facility. We would like to thank S. Aubry and A. R. Bishop for useful discussions, and Y. S. Kivshar and D. K. Campbell for communicating their work prior to publication. The authors thank CEC for financial support, Contract No. SC1-CT91-0705, and NATO Grant No. 95 920468. The Laboratoire de Physique is "Unité de Recherche Associée au Centre National de la Recherche Scientifique No. 1325."

[1] A. R. Bishop, *Solitons and Condensed Matter Physics*, edited by A. R. Bishop and Y. Schneider (Springer, Berlin, 1979).
[2] W. P. Su, J. R. Schrieffer, and A. J. Heeger, Phys. Rev. B **22**, 2099 (1980).
[3] V. Antonchenko, A. S. Davydov, and A. V. Zolotaryuk, Phys. Status Solidi B **115**, 631 (1983).
[4] A. S. Davydov, Phys. Scr. **20**, 387 (1979).
[5] M. Peyrard and A. R. Bishop, Phys. Rev. Lett. **62**, 2755 (1989).
[6] T. Dauxois, M. Peyrard, and C. R. Willis, Physica D **57**, 267 (1992).
[7] J. A. Combs and S. Yip, Phys. Rev. B **28**, 6873 (1983).
[8] R. Boesch and C. R. Willis, Phys. Rev. B **39**, 361 (1989).
[9] R. Boesch, C. R. Willis, and M. E. Batanouny, Phys. Rev. B **40**, 2284 (1989).
[10] R. Boesch and M. Peyrard, Phys. Rev. B **43**, 8491 (1991).
[11] R. Scharf and A. R. Bishop, Phys. Rev. A **43**, 6535 (1991).
[12] Y. S. Kivshar and D. K. Campbell (unpublished).
[13] D. Cai, A. R. Bishop, and N. Grønbech-Jensen (unpublished).
[14] A. J. Sievers and S. Takeno, Phys. Rev. Lett. **61**, 970 (1988).
[15] S. Takeno, K. Kisoda, and A. J. Sievers, Prog. Theor. Phys. Suppl. **94**, 242 (1988).
[16] R. Bourbonnais and R. Maynard, Phys. Rev. Lett. **64**, 1397 (1990).
[17] Y. S. Kivshar, Phys. Lett. A **161**, 80 (1991).
[18] M. Peyrard and M. D. Kruskal, Physica D **13**, 88 (1984).
[19] M. Peyrard, St. Pnevmatikos, and N. Flytzanis, Phys. Rev. A **36**, 903 (1987).
[20] M. Remoissenet, Phys. Rev. B **33**, 2386 (1986).
[21] A. Seeger and P. Schiller, in *Physical Acoustics*, edited by W. P. Mason (Academic, New York, 1966), Vol. III-A.
[22] D. K. Campbell and M. Peyrard, in *Chaos*, edited by D. K. Campbell (AIP, New York, 1990), p. 305.
[23] T. Dauxois, M. Peyrard, and A. R. Bishop, Phys. Rev. E **47**, 684 (1993).
[24] O. M. Braun and Y. S. Kivshar, Phys. Rev. B **43**, 1060 (1991).
[25] A. A. Maradudin, E. W. Montroll, G. H. Weiss, and I. P. Ipatova, *Theory of Lattice Dynamics in the Harmonic Approximation* (Academic, New York, 1971).
[26] S. Nosé, Mol. Phys. **52**, 255 (1984).
[27] Y. S. Kivshar and M. Peyrard, Phys. Rev. A **46**, 3198 (1992).
[28] S. Takeno, J. Phys. Soc. Jpn. **61**, 2823 (1992).
[29] J. Pouget, M. Remoissenet, and J.M. Tamga, Phys. Rev. B **47**, 14 866 (1993).